Supporting Information

Facile Synthesis and Electronic Structure Optimization of Sub-nanometer Palladium Clusters for Efficient Direct Synthesis of H_2O_2

Yulu Chen[a,b], Hongyan Pan[a,b], Chunliang Yang[a,b], Haipeng Xiao[a,b], Zheng Chen[a,b]*, Chun Zhu[a], Weiyue Zhao[a,b]*, Qian Lin[a,b]*

[a] School of Chemistry and Chemical Engineering, Guizhou University, Guiyang, Guizhou 550025, China.

[b] Guizhou Key Laboratory of Green Chemical and Clean Energy Technology, Guiyang, Guizhou 550025, China

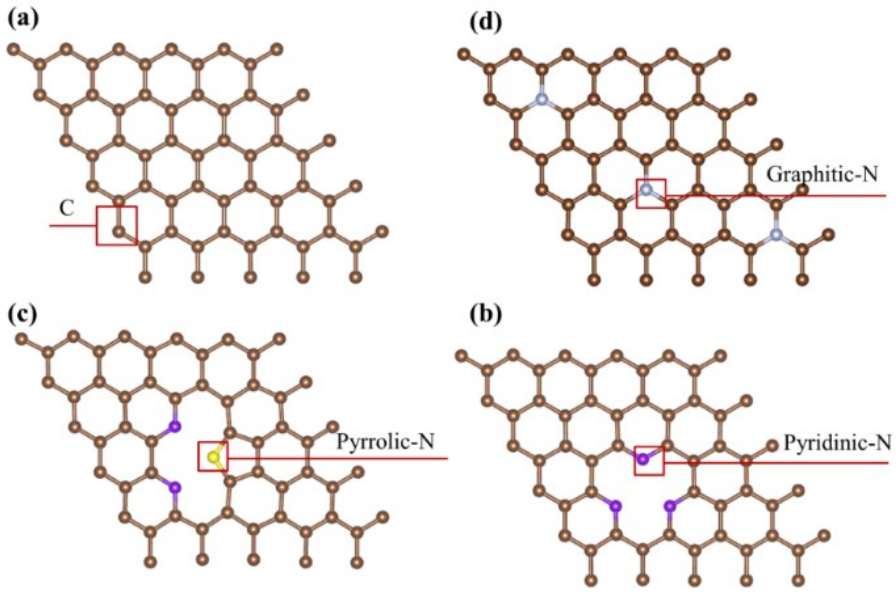

Figure S1. The models of (a) graphitic, (b) graphitic doped with Pyridinic-N, (c) graphitic doped with Pyrrolic-N and (d) graphitic doped with Graphitic-N.

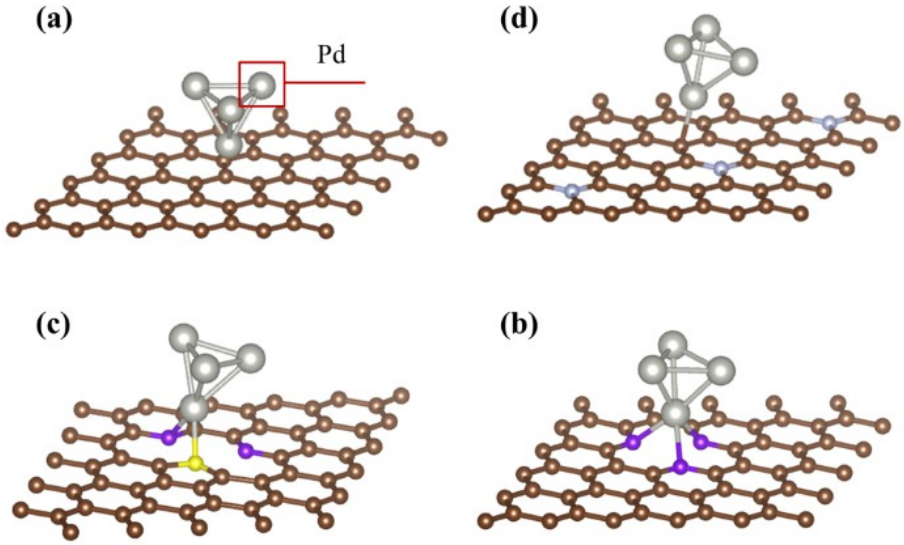

Figure S2. (a) The optimized models of Pd cluster adsorbed on (a) graphitic, (b) graphitic doped with Pyridinic-N, (c) graphitic doped with Pyrrolic-N and (d) graphitic doped with Graphitic-N.

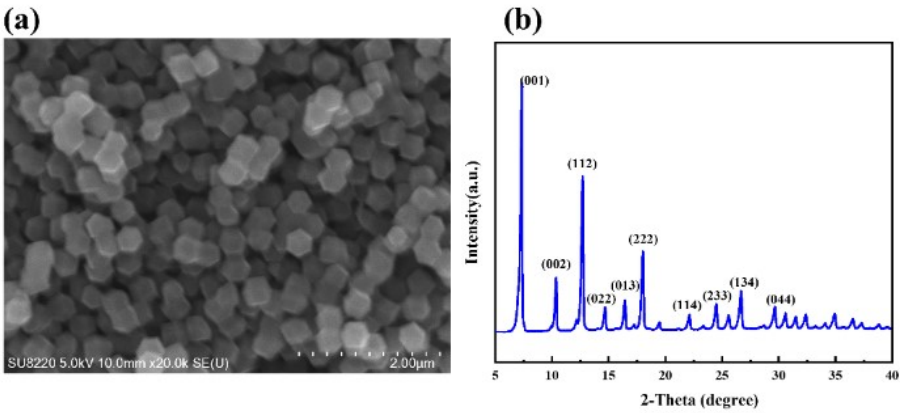

Figure S3. (a) SEM image of ZIF-8; (b)XRD spectra of ZIF-8

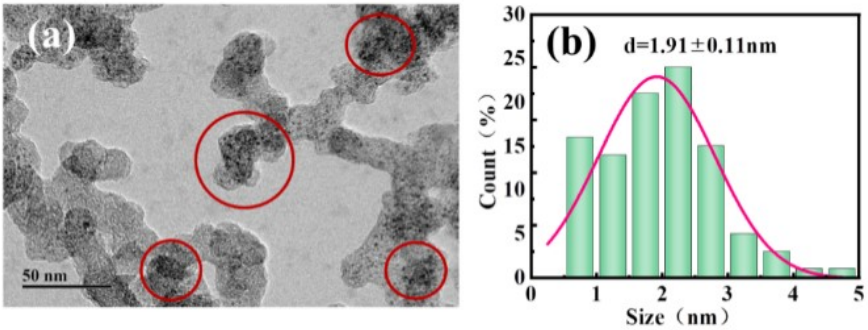

Figure S4. (a) TEM images of Pd/ XC-72. (b) Pd NPs size distribution of Pd/ XC-72.

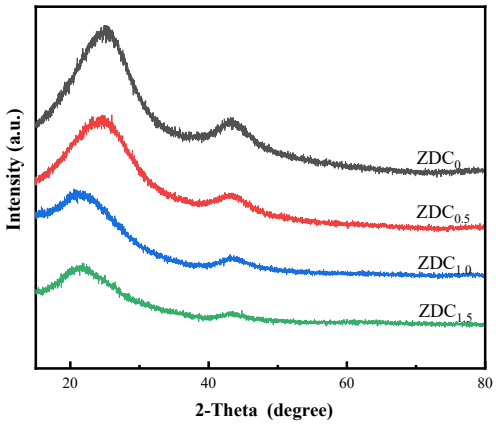

Figure S5. XRD spectra of ZDC_X.

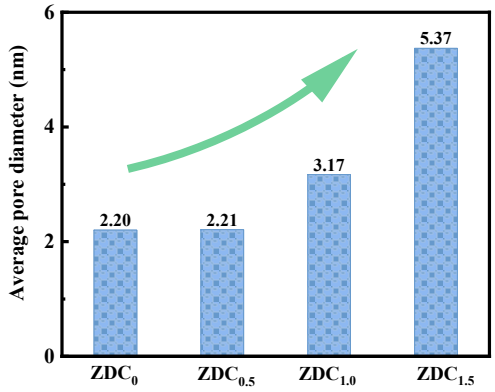

Figure S6. Average pore diameter of ZDC_X.

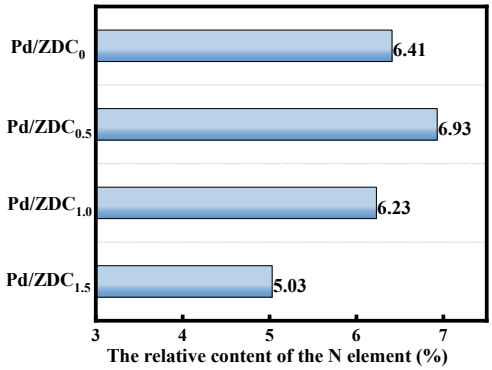

Figure S7. The relative content of the N element of ZDC_0, $ZDC_{0.5}$, $ZDC_{1.0}$ and $ZDC_{1.5}$

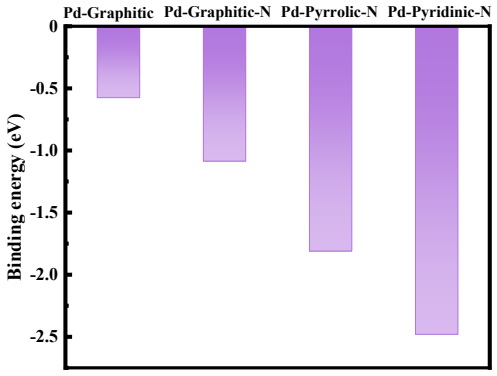

Figure S8. Binding energy of Pd cluster adsorbed on pristine graphitic and graphitic doped with graphitic-N, pyrrolic-N and pyridinic-N.

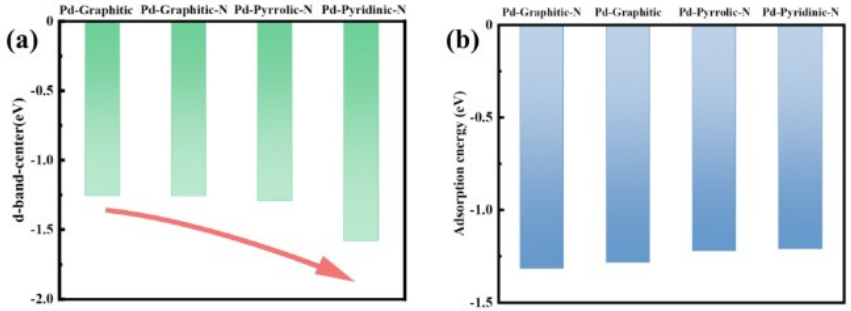

Figure S9. (a) The d-band-center of Pd cluster adsorbed on graphitic and graphitic doped with graphitic-N, pyrrolic-N and pyridinic-N. (b) Adsorption energy of O_2 on Pd-Graphitic, Pd-Graphitic-N, Pd-pyrrolic-N and Pd-pyridinic-N

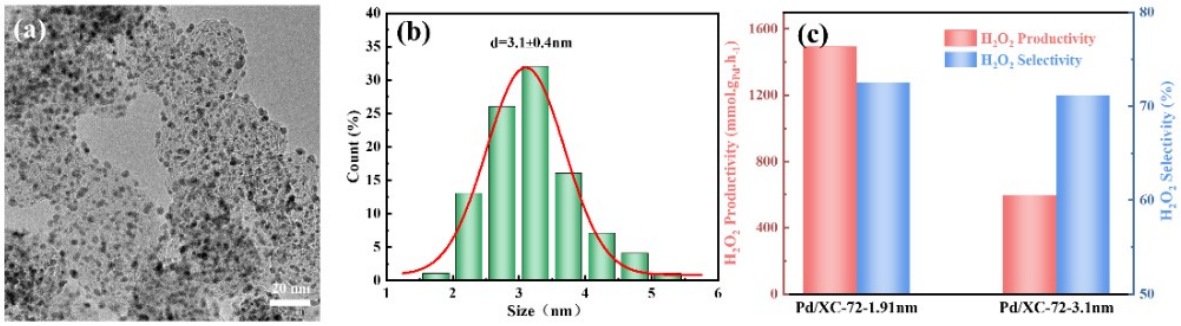

Figure S10. (a) TEM image of Pd/XC-72-3.1nm, (b) Pd NPs size distribution of Pd/XC-72, (c) evaluation results of catalytic performance of Pd/XC-72-1.91nm and Pd/XC-72-3.1 nm.

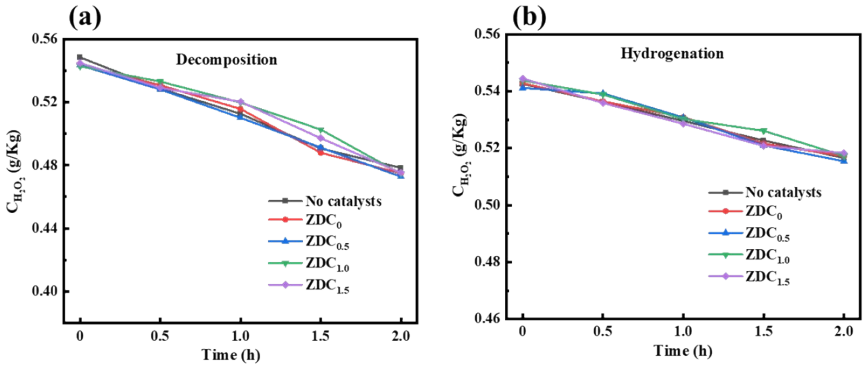

Figure S11. (a) H_2O_2 decomposition and (b) hydrogenation test for ZDC_X carriers.

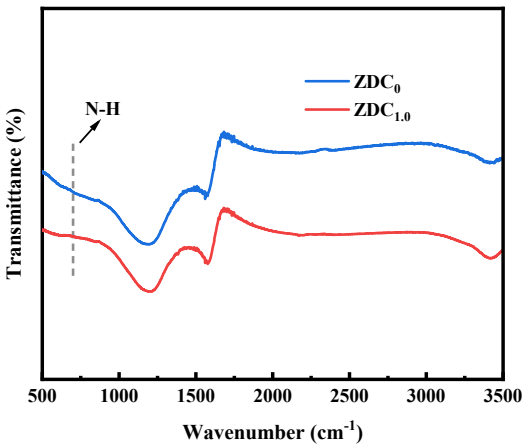

Figure S12. FTIR spectra of ZDC_0 and $ZDC_{1.0}$.

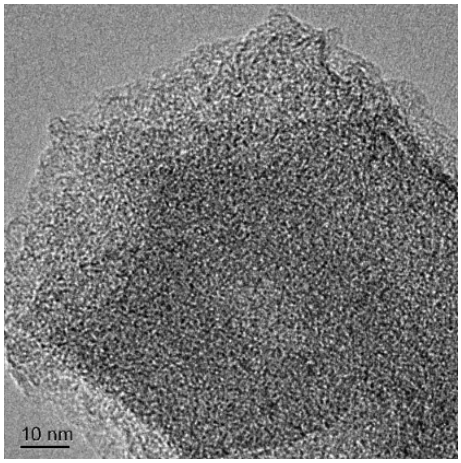

Figure S13. TEM of Pd/ $ZDC_{1.0}$ catalyst after four cyclic experiments

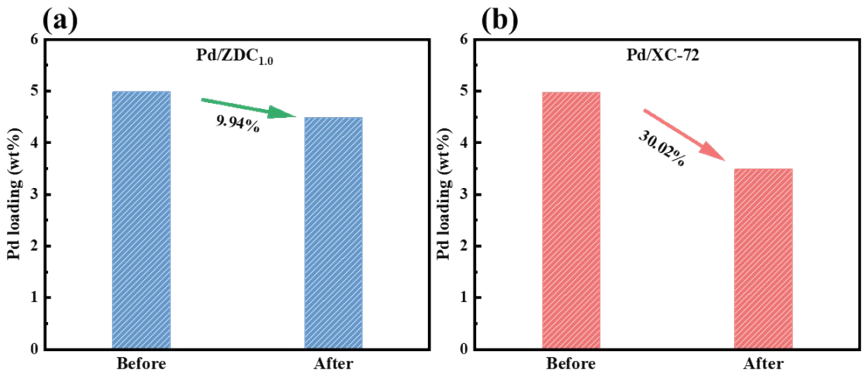

Figure S14. The Pd leaching rate of catalysts after cycling experiments, (a) Pd/$ZDC_{1.0}$, (b) Pd/XC-72.

Table S1 The Pd loading of catalysts measured by ICP-AES

catalysts	theoretical Pd loading (wt%)	actual Pd loading (wt%)	residual Zn (wt%)
Pd/ZDC_0	5.0	4.865	N/A
$Pd/ZDC_{0.5}$	5.0	4.902	N/A
$Pd/ZDC_{1.0}$	5.0	4.934	N/A
$Pd/ZDC_{1.5}$	5.0	4.896	N/A
Pd/XC-72	5.0	4.878	/

Δ: N/A indicates that no corresponding element has been detected.

Table S2. Structural parameters of ZDC_X.

catalyst	S_{BET} (m^2/g)	V_{mic} (cm^3/g)	V_{mes} (cm^3/g)
Pd/ZDC_0	1230.51	0.44	0.24
$Pd/ZDC_{0.5}$	1845.97	0.61	0.41
$Pd/ZDC_{1.0}$	2964.64	0.75	1.60
$Pd/ZDC_{1.5}$	3088.89	0.82	3.32